Journal of Energy & Environment 3 (2004) 33 - 47

Evaluation of Different Types of Friction to Improve the Performance of a Direct Injection Diesel Engine

Nafis Ahmad-1, Abhishek Nandy and Shefali Gaur
Mechanical Engineering Department, Aligarh Muslim University
Aligarh (U.P.) -202002, India
Email: drnafis_ahmad@yahoo.com
(Received on 27 Aug 2000, revised on 15 Feb 2004)

Abstract

The availability of high performance computers enables us to simulate the effect of engine parameters on performance of an engine. The simulation is useful in optimizing the engine performance for various engine parameters. Further, it saves time and cost, and helps in reducing the number of variables that need to be studied experimentally. This paper studies the effect of friction power on the engine performance characteristics of a diesel engine by varying different engine parameters such as engine speed (800 – 2400 rev/min), fuel air equivalence ratio (0.5 – 0.8), compression ratio (14 – 24) and injection timing (10 – 50 deg before top dead centre). A thermodynamic computer simulation model based on Double Wiebe Function has been considered. The optimization is done with an attempt to reduce friction power and thus increase the engine brake power.

Nomenclature

AP	area of cross section of piston
BP	brake power
CR	compression ratio
D	bore of the engine cylinder
DTHD	heat release (diffusion burning)
QDTHP	heat release (premixed burning)
IMEPC	indicated mean effective pressure during compression
IVD	inlet valve diameter
L	length of connecting rod
LP	piston skirt length
P	initial pressure
Pa	ambient pressure
PEM	exhaust back pressure
Ps	suction pressure
S	stroke length
τ	torque
THETAD	diffusion burning duration
THETAP	premixed burning duration
V	volume of cylinder
Vp	piston speed
XMD	seat liberated (diffusion burning)
XQP	heat liberated (premixed burning)
SP	suction pressure, bar
Vcl	clearance volume
XMP	shape factor during premixed combustion
THETA1	angle controlling premixed combustion

EXP	exponential
QD	heat release during diffusion burning
Q_i	heat transfer rate for a particular surface
h_i	heat transfer coefficient for any surface
Ai	area of any surface
Tg	temperature of gas
T_{wi}	temperature of wall for any surface
h	heat transfer coefficient
DE	change in internal energy
F	equivalence ratio
M	total mass
R	gas constant
N_p	number of piston rings (=2)
N	engine speed (rev/min)
WD	work done
TDC	top dead centre
BTDC	before top dead centre
BDC	bottom dead centre
ABDC	after bottom dead centre
BBDC	before bottom dead centre
CA	crank angle (degrees)
T	cylinder temperature
C11, C12	constants for air
C13, C14, C15	

Values of Constants

C_{11}	0.6919943
C_{12}	$-0.3917296 * 10^{-4}$
C_{13}	$0.5292534 * 10^{-7}$
C_{14}	$0.2286286 * 10^{-10}$
C_{15}	$0.2775890 * 10^{-14}$

Introduction

Combustion in a diesel engine is a complicated process. Accurate description of this process is rather difficult as it involves a number of physio-chemical effects occurring simultaneously which are not very well understood even now. During combustion one or more jets of fuel are injected into the combustion chamber where air is present at high temperature and pressure. As the droplets of fuel enter the hot air, they are surrounded by their own vapour, which in turn is inflamed at the surface of envelope.

Mainly eight models have so far been proposed in literature [1-8] to simulate the engine performance. They can be categorized as thermodynamic single zone [1-4] and thermodynamic multi zone [5-8] models. Brief descriptions of the models are as follows.

<u>Wiebe's Model</u> [1]:

A form of burning rate curve suggested by Wiebe on consideration of chemical kinetics has been found to give satisfactory heat release pattern in cycle calculations.

<u>Lyn's Model</u> [2]:

A triangular pattern of heat release was adopted by Lyn with the assumption that the heat release occurred over a period of 40-50 degrees of crank angle.

Krieger and Borman [3]:

By application of the first law of thermodynamics, and equation of states, the researchers analyzed the cylinder pressure diagrams to determine the rate of heat release. The heat release rate diagram so obtained was assumed as input data to the cycle simulation program.

Austen and Lyn [4]:

An empirical burning law has been derived to correlate the rate of heat release with the rate of injection. The model was based on single droplet combustion theory suitably modified to take into account the effect of depletion of oxygen in the cylinder due to combustion of fuel.

Whitehouse and Way [5]:

They introduced the concept of two zone combustion models for the medium and high-speed engines.

Grig and Syed [6]:

A two-zone model was developed to calculate the rate of heat release in a direct injection diesel engine. This model considered the rate of air entrainment into the fuel spray, the rate of turbulent mixing of the fuel and air within the spray and the chemical kinetics of burning.

Kumar et al [7]:

A single and a two-zone model were developed. In the single zone model, the researchers have taken into consideration the rate of preparation and the rate of burning to calculate the heat release rate, whereas in the two-zone model they have utilized an air entrainment model based on spray penetration and a fuel preparation model.

Matsuoka et al [8]:

They developed a stratified three-zone combustion model consisting of a burning zone, a burned zone and a low temperature zone based on the hypothesis of burned gas re-entrainment into the diesel spray flame.

In this paper a thermodynamic computer simulation model based on Double Wiebe Function [1,9,10] has been considered. This studies the effect of friction power on the engine performance characteristics of a diesel engine by varying different engine parameters such as engine speed, fuel air equivalence ratio, compression ratio and injection timing.

Mathematical Model

The engine develops the power during the expansion stroke, which is assumed to start from the inlet valve closing to the exhaust valve opening. The assumptions that have been made in developing the in-cylinder model for direct injection diesel engine are as follows.

1. The pressure and temperature are uniform throughout the cylinder.
2. The unburnt mixture at any instant consists of air and residual gases without any chemical reaction.
3. The heat transfer area consists of three main surfaces namely, the cylinder head, the piston top and the instantaneous sleeve surface.
4. The metal temperature of each of the above-mentioned surfaces is constant throughout the cycle.
5. The rate of heat transfer from gases to the wall is calculated from the instantaneous heat transfer coefficient, in temperature between the gas and wall.

Mathematical Equations Used [9]

(A) Cylinder volume

The cylinder volume at any instant of crank angle can be obtained by using the equation of crank slider mechanism and from the engine geometry. The instantaneous total volume of gases in the cylinder is given as:

$$V = Vcl + Ap + [L + \left(S/2\right)\left(1-\cos\theta\right) - \left\{L^2 - \left(S^2/4\right)\sin^2\theta\right\}^{1/2}] \quad (1)$$

where θ is the crank angle measured with respect to top dead center in radians.

(B) Heat release during premixed burning

$$QDTHP = 6.9 * \left(XQP/THETAP\right) * \left(XMP+1\right) * \left(THETA1/THETAP\right)^{XMP} * EXP\left[6.9 * \left(THETA1/THETAP\right)^{(XMP+1)}\right] \quad (2)$$

where,

XMP=3.0
XMD=0.9
THETAP=7^{o} CA [Heat release during premixed burning].

(C) Heat release during diffusion burning

$$DTHD = 6.9 * \left(QD/THETAD\right) * \left(XMD+1\right) * \left(THETA1/THETAD\right)^{XMP} * EXP\left[-6.9 * \left(THETA1/THETAD\right)^{(XMP+1)}\right] \quad (3)$$

THETAD=90^{o} CA [Heat release during diffusion burning]

(D) Heat transfer

The heat transfer rate for any surface at a particular instant can be determined by the equation :

$$Qi = hi * Ai * \left(Tg - Twi\right) \quad (4)$$

Gas to wall heat transfer in the engine cylinder of a C.I engine is controlled by a rapidly changing boundary layer caused by gas motion due to piston movement and geometry of combustion chamber. Hohensberg's correlation [10] is the most adequate among all available relations, to compute the heat transfer rate through cylinder. Equation (5) shows this.

$$h = 130 * V^{-0.06} * P^{0.8} * T^{0.4} * \left(Vp + 1.4\right)^{0.8} \quad (5)$$

(E) Change in internal energy

The internal energy is calculated using the empirical relation given as

$$DE = \left(C_{11} + 2*C_{12}*T + 3*C_{13}*T^2 + 4*C_{14}*T^3 + 5*C_{15}*T^4\right)*1000 \tag{6}$$

$$\dot{T} = \frac{Z_1 - \dot{F}\left(\partial u/\partial F\right) - \left(P/Z_2\right)\left(\partial u/\partial P\right)\left\{\dot{M}/M - \dot{V}/V + \left(\dot{F}/R\right)\left(\partial R/\partial F\right)\right\}}{\left\{\left(\partial u/\partial T\right) + \left(P/T\right)\left(\partial u/\partial P\right)\left(Z_3/Z_2\right)\right\}} \tag{7}$$

where,

$$Z_1 = -RT\left(\dot{V}/V\right) + \left(1/M\right)\left(\Sigma \dot{Q}_i + \Sigma h_i Mi - u\dot{M}\right)$$
$$Z_2 = 1 - \left(P/R\right)\left(\partial P/\partial R\right)$$
$$Z_3 = 1 + \left(T/R\right)\left(\partial T/\partial R\right)$$

This derivative of temperature holds good for all in-cylinder processes except the combustion process where in a different set of relation have been developed. This equation can be solved for the gas temperature by suitable numerical integration in conjunction with the equation for heat transfer, mass flow rate and volume change. It is also necessary, all the time, to keep a track of the changing mixture composition in the cylinder to derive the property relation of gas constant and internal energy.

Evaluation of Friction Power [11]

Part of the power developed in the cylinder of an IC engine is absorbed to overcome friction in the various parts, inlet and throttling losses and pumping losses.

The following empirical relations have been used for the prediction of various types of friction prevailing inside the diesel engine for its wide engine operating range (CR, N).

Friction due to gas pressure behind the piston rings:

FP_1=0.0042*(Pa-Ps)*(S/D^2)*[0.0888 *CR +0.182*(CR**(1.33-0.394*V_P/100))] (8)

Friction due to wall tension of rings:

FP_2 = 0.003697 * S * N_P / D^2 (9)

Friction due to piston and rings:

FP_3 = 0.000126 * L_P * V_P / (D * S) (10)

Friction due to blow by loss:

FP_4=0.99034*(Pa-Ps)$^{0..5}$*[0.121*CR$^{0.4}$-0.0345+0.001055*CR)* (N/1000)$^{1.185}$] (11)

Inlet and throttling loss:

$$FP_5 = (P_{em} / 2.75) + Ps \tag{12}$$

Friction due to valve gear:

$$FP_6 = 7.0083*10^{-4}*[30-(4* N/1000)] *(IVD)^{1.75} / (D^2*S) \tag{13}$$

Pumping loss:

$$FP_7 = 0.02696 * (N / 1000)^{1.5} \tag{14}$$

Bearing friction loss:

$$FP_8 = 0.055307 * (D / S) * (N / 1000) \tag{15}$$

Combustion chamber and valve pumping loss:

$$FP_9 = 0.0915 * (IMEPc / 11.67)^{0.5} *(N / 1000)^{1.7} \tag{16}$$

where,

$V_p = S * N / 30$

$IMEPc = 4 * WD / (PI * D^2 * S)$

$WD = 60 * POWER / N$

Total frictional power (kW):

$$TFP = FP_1+FP_2+FP_3+FP_4+FP_5+FP_6+FP_7 + FP_8 + FP_9 \tag{17}$$

Brake power (kW) is expressed as:

$$BP = POWER - TFP \tag{18}$$

Torque (N-m) is evaluated as:

$$\tau = BP * 60 * 1000 / (2 * PI *N) \tag{19}$$

The mechanical efficiency (%) is given by:

$$\eta_m= (BP / POWER) * 100 \tag{20}$$

Results and Discussion

The results obtained from the computer simulation model [12] including a comparison with the computed and available experimental data are presented and discussed below. The specifications of the engine studied are given in the Appendix.

Fig. 1 shows the comparison between experimental and predicted cylinder pressure diagram with respect to crank angle for an engine speed of 1700 rev / min. and injection timing 14 ^{o} BTDC. The irregularities shown in the diagram may be caused due to vaporization of diesel fuel with cylinder walls causing cooling effect that affects the pressure and temperature trend. The comparison shows good agreement between experimental and theoretical results.

Fig. 2 shows the variation of computed cylinder temperature with respect to crank angle for the same engine operating conditions. During combustion the temperature is rising and afterwards it falls following expansion of the burnt gases and producing work output.

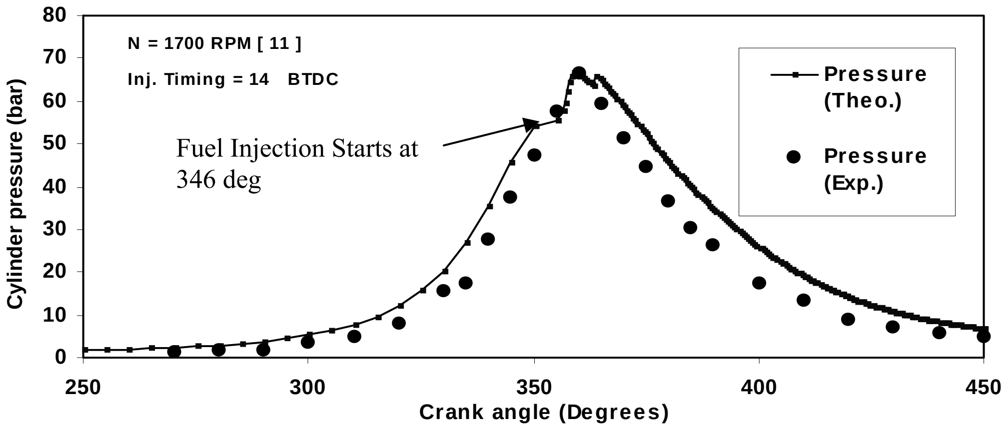

Fig. 1 Shows the comparison between computed and experimental pressure crank angle diagram

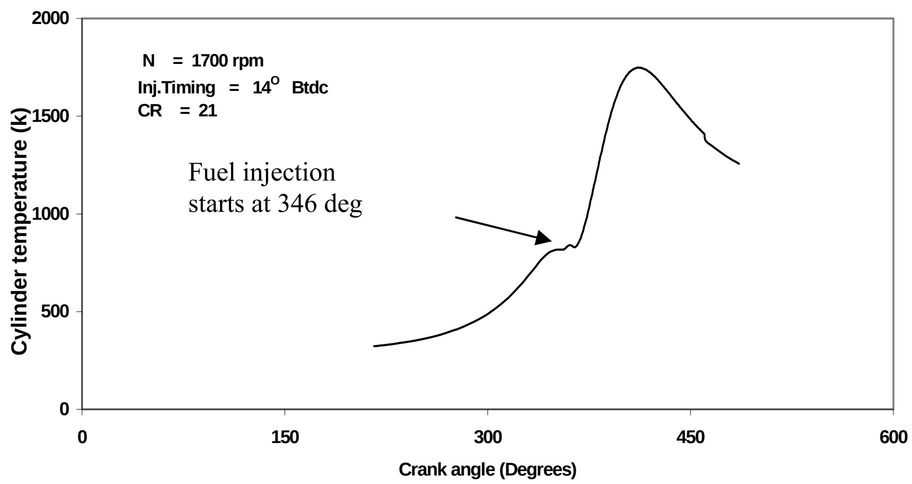

Fig. 2 Shows the variation of crank angle with cylinder temperature

Fig. 3 shows the variation of total friction power, indicated power and brake power with engine speed. The total friction power increases with an increase in engine speed, which is quite evident from the graphical representation. The trend is also same for brake power and indicated power. As the speed increases, the engine consumes more amount of the fuel, which increases the brake power and indicated power. The friction power also increases due to more frictional losses of moving and reciprocating parts encountered by higher engine speed.

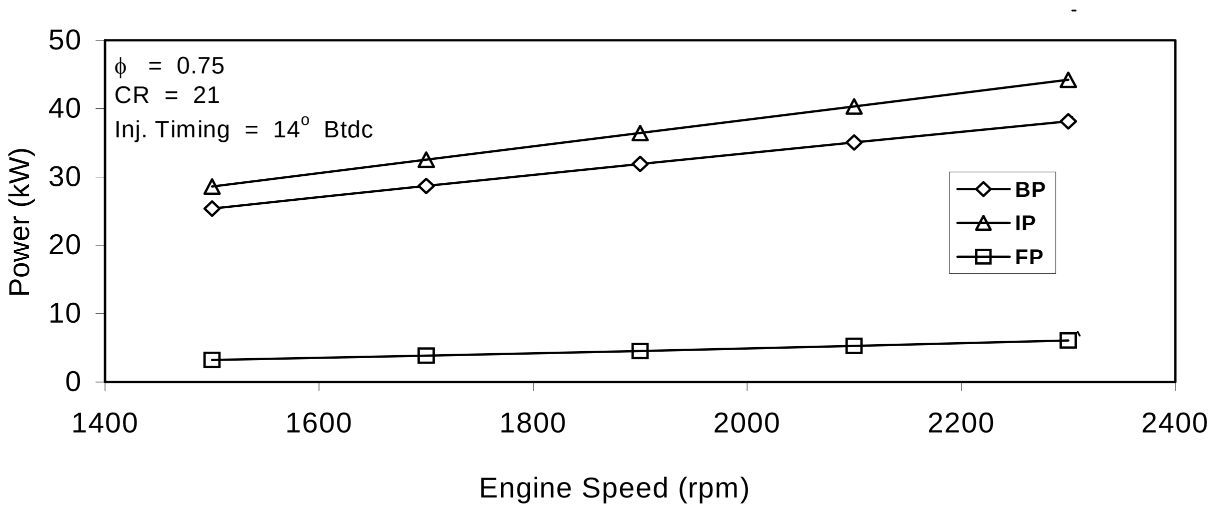

Fig, 3 Shows the variation of power with engine speed

Fig. 4 shows the variation of various friction powers with respect to engine speed. It can be seen from the graph that frictions in certain parts of an engine increase with an increase in engine speed and also remain approximately same in certain other parts of the engine. The increasing trend is found in case of combustion chamber and valve pumping loss. It is due to increase in indicated mean effective pressure with engine speed. Although in other cases the friction loss is not so prominent.

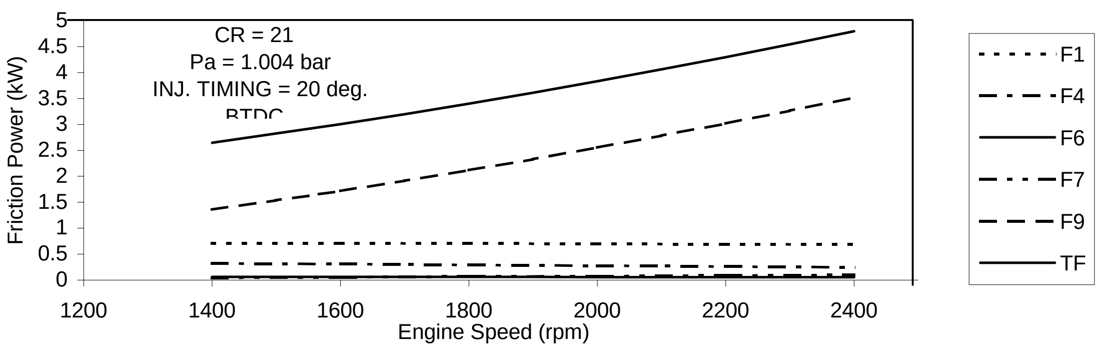

Fig. 4 shows the variation of different friction powers with engine speed

Fig. 5 shows the variation of experimental results of brake specific fuel consumption and brake thermal efficiency for an engine speed of 1700 rev/min, compression ratio 21 and injection timing of 20 degrees btdc with respect to engine brake power. From the graph it is seen that the brake thermal efficiency is maximum where the specific fuel consumption is minimum.

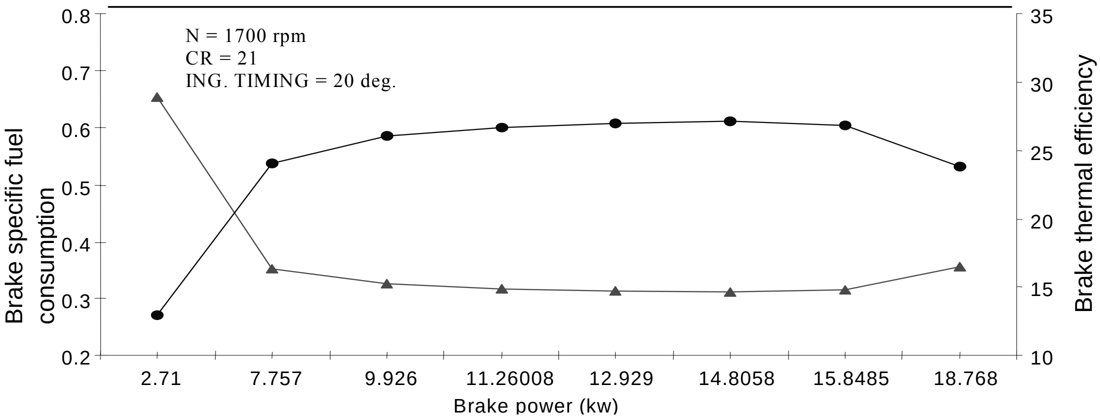

Fig. 5 Shows the variation of brake specific fuel consumption thermal efficiency

Fig. 6 shows the variation of mechanical efficiency and engine torque with engine speed. It can be observed that with an increase in engine speed the mechanical efficiency first displays an increasing trend followed by a decreasing trend after an optimum value of engine speed. It is due to the reason that as the engine speed increases the internal friction of the air entering the cylinder increases, which reduces the volumetric efficiency and also the mechanical efficiency. With an increase in engine speed, an increase in engine torque is observed, but the variation is not linear and the increase in torque developed drops with increasing engine speed. It is due to higher mechanical losses prevailing at higher engine speeds.

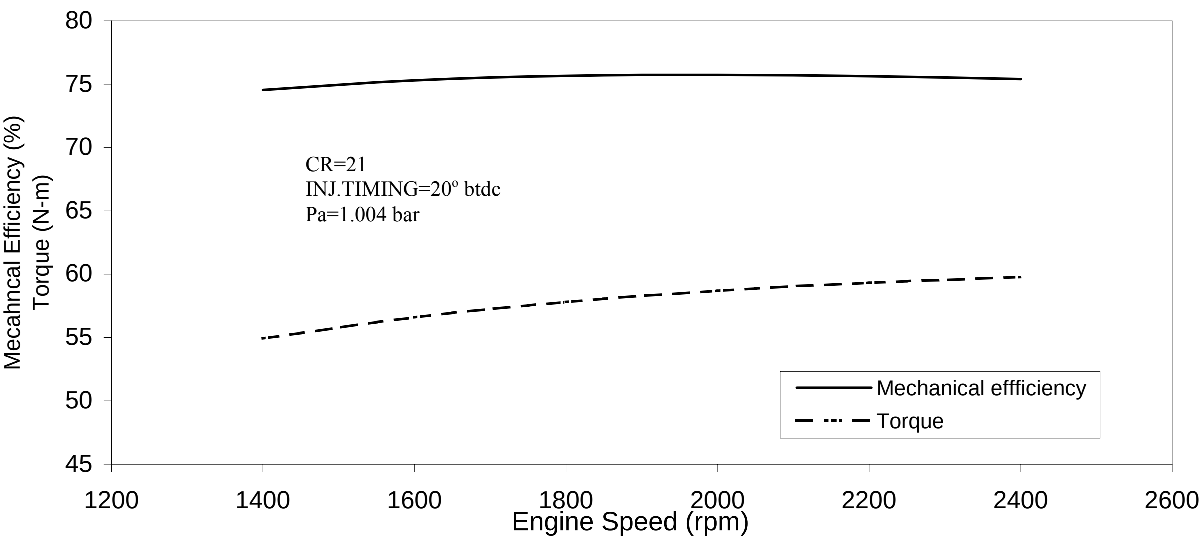

Fig. 6 Shows the variation of mechanical efficiency with respect to engine speed

Fig. 7 shows the variation of work done with respect to engine speed for different injection timings. With an increase in engine speeds the work done increases. It is seen from the graph that for the injection timing 40^o btdc the work done is maximum and for 10^o btdc it is minimum. If the injection timing is retarded too long, by the time the combustion process is complete the piston is still reaching toward TDC and very little energy would be available on the piston to move it downward for power stroke and so developing a less power. Although for injection timing 40^o BTDC, by the time the piston moves downwards towards BDC, the combustion is about to complete and all the energy released would be utilized to push the piston downward on power stroke, thus increasing the power output of the engine.

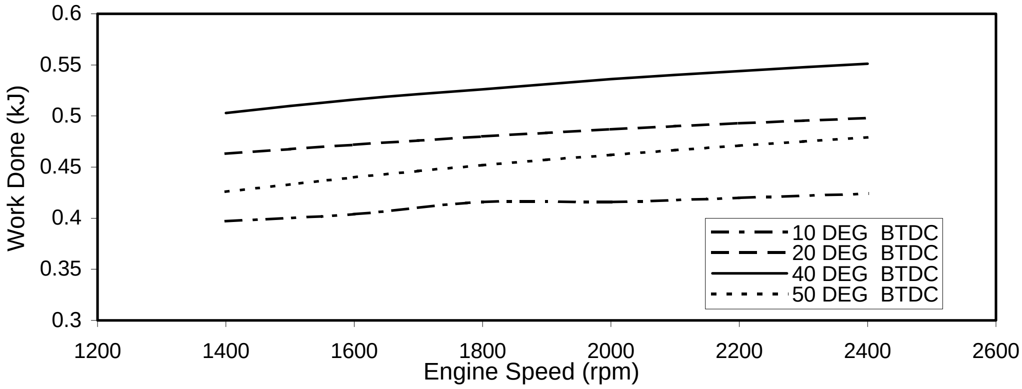

Fig. 7 Shows the variation of work done with respect to engine speed at different injection timings

Fig. 8 shows the variation of total friction power with engine speed for different injection timings (20, 40 and 50^o BTDC). As seen from the graph, there is not a much effect of injection timing on the total friction power. However a small variation is observed at high engine speed. Although, there is a slight increase in the total friction power with increase in injection timing till 40^o btdc after which it drops.

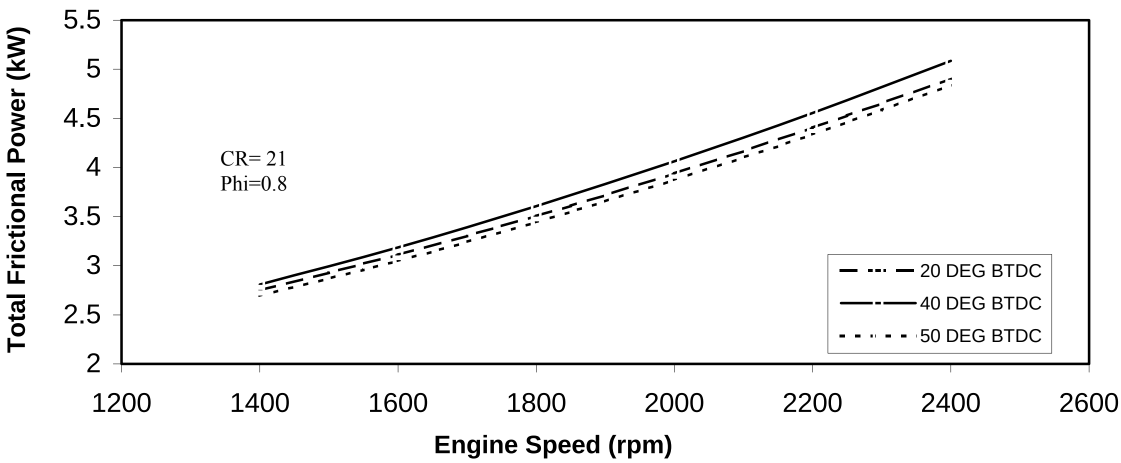

Fig. 8 Shows the variation of total frictional power with respect to engine speed at different injection timings

Fig. 9 shows the variation of indicated power with respect to engine speed for different injection timings. There is a small increase in the indicated power with increase in injection timing. The indicated power is maximum for 40^o and minimum for 50^o BTDC. For injection timing 20^o BTDC it lies in between the two.

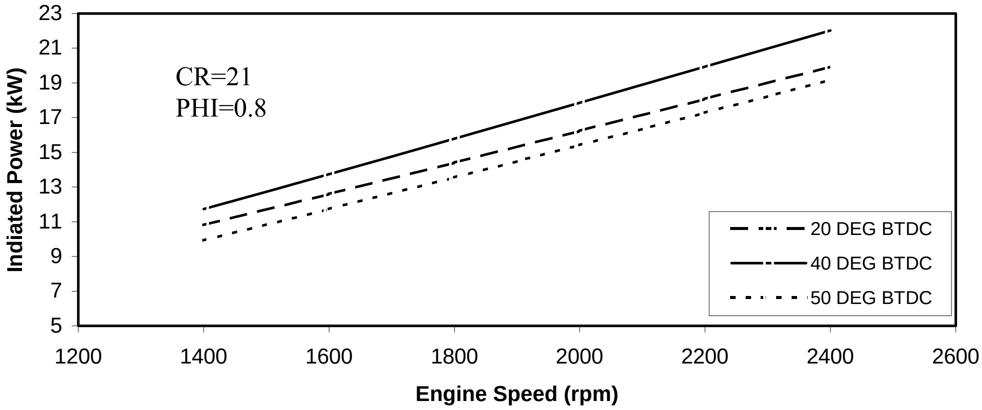

Fig. 9 Shows the variation of indiacated power with respect to engine speed at different injection timings

Fig. 10 shows the effect of engine speed on torque developed for varying injection timings from 20^o BTDC to 50^o BTDC. From the figure, it is evident that the torque developed increases with increase in injection timing till 40^o after which it drops exceptionally for the above-explained same reason.

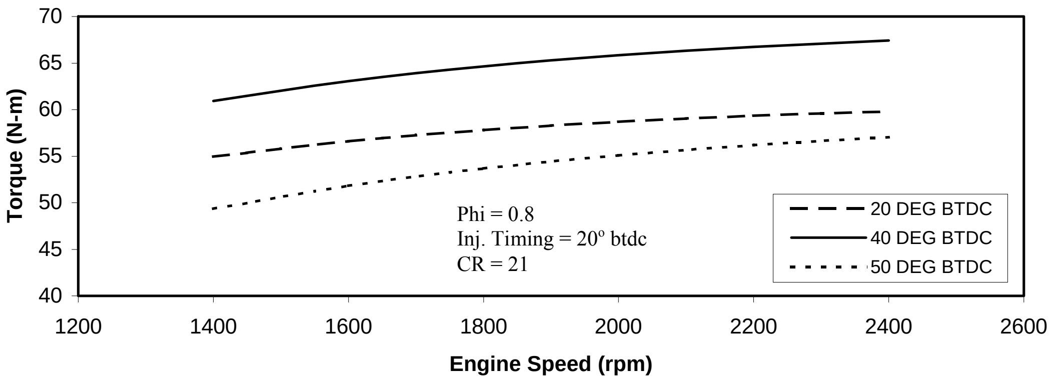

Fig. 10 Shows the variation of torque with respect to engine speed at different injection timings

Fig. 11 shows the variation of brake power with engine speed for different injection timings. Graph shows that the brake power increases with an increase in engine speed and is maximum for injection timing of 40^o btdc for the same above-mentioned reason.

Fig. 12 also depicts the same trend for mechanical efficiency with respect to engine speed. The mechanical efficiency increases with an increase in injection timing till 40^o btdc after which it decreases. If injection timing is further retarded then all the energy released during combustion will not be utilized by the time the exhaust valve opens. Most of the energy would be exhausted to the environment causing an increase in air pollution. If it were advanced further, the energy released would not be utilized to push the piston as the piston is still in upward motion. It is also possible that the engine can stall. The efficiency also increases with an engine speed and afterwards decreases it is due to prevailing higher mechanical losses inside the engine parts.

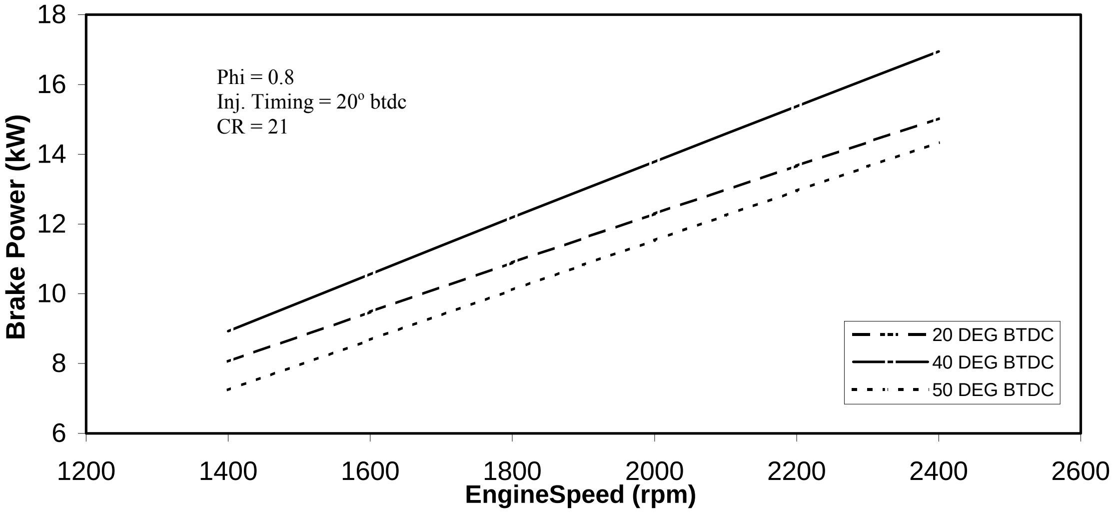

Fig. 11 Shows the variation of brake power with respect to engine speed at different injection timings

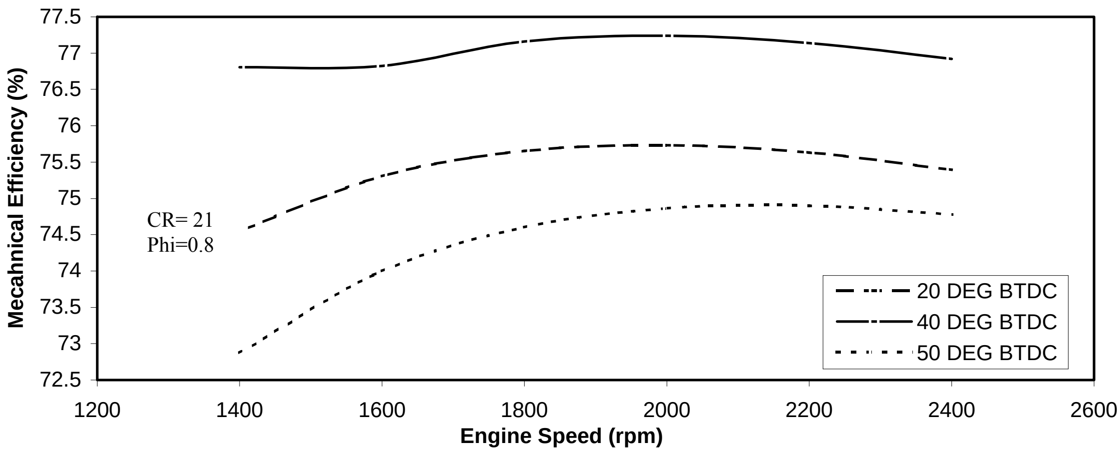

Fig. 12 Shows the variation of mechanical efficiency with respect to various engine speed at different injection timings

Fig. 13 shows the variation of indicated power with engine speed for varying equivalence ratio. The indicated power increases with the increase in equivalence ratio and the rise is more at higher engine speed. It is due to a richer mixture burnt inside the engine cylinder.

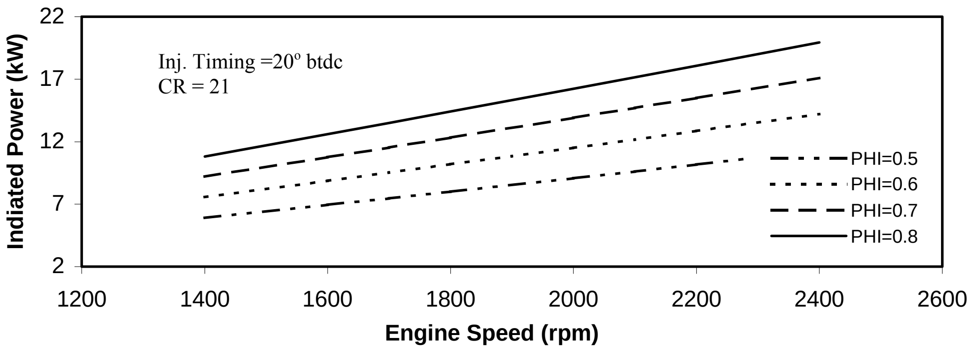

Fig. 13 Shows the variation of indiacated powe with respect to engine speed at different equivalence ratio

Fig. 14 shows the effect of indicated mean effective pressure during compression with compression ratio for varying injection timings. From the graphical representation it can be concluded that the indicated mean effective pressure during compression increases with increasing injection timing. Although at injection advance of 50° btdc the indicated mean effective pressure decreases. At a compression ratio of 22, a dip is observed although at compression ratio 24 the normal trend is exhibited.

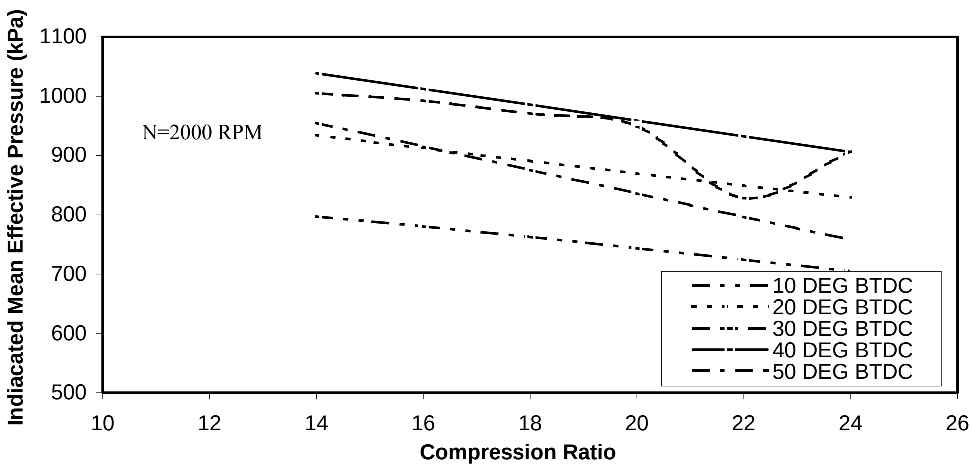

Fig. 14 Shows the variation of indicated mean effective pressure with respect to compression ratio at different injection timings

It could be due to abnormal combustion which might limit the range of operation of the engine under the given compression ratio for a particular injection timing. As the energy released during combustion is not fully utilized because the piston is still reaching towards TDC position. The indicated mean effective pressure is a measure of indicated power relative to its size. Higher mean effective pressure means increased cylinder pressure and temperature, greater stress on the engine structure and reciprocating components and increased potential to knock.

Fig. 15 shows the variation of total friction power with injection timing for an engine speed of 2000 rev/min and compression ratio 21. For injection timings varying from 10^o to 40^o BTDC, an increasing trend of total friction power is obtained which thereafter drops sharply as the injection timing is further retarded. Because the combustion still continues by the time the exhaust valve opens.

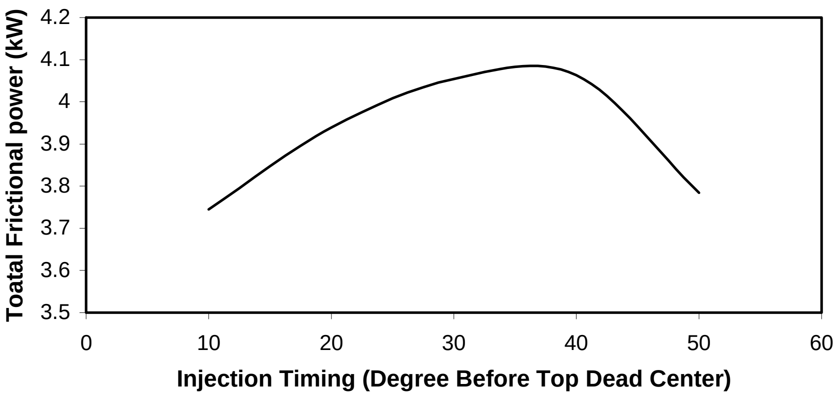

Fig.15 Shows the variation of toatal frictional power with respect to injection timings

The simulation results show that maximum values of indicated power, brake power, torque, mechanical efficiency, work done, and indicated mean effective pressure during compression are obtained for the following engine operating conditions as given in Tables 1 and 2.

Table 1 Simulated and optimized engine-operating parameters to give maximum engine output

Engine parameters	**Optimum Values**
Engine speed	2400 rpm
Ambient pressure	1 bar
Injection timing	40 ° BTDC
Equivalence ratio	0.8

The minimum friction power is achieved with the following engine parameters:

Table 2 Simulated and Optimized values giving minimum friction power

Engine Parameters	Optimum values
Compression Ratio	14
Ambient pressure	1 bar
Injection Timing	10 ° BTDC
Engine speed	1400 rpm

Conclusions

This paper demonstrates how one can use thermodynamics modeling techniques to evaluate the performance of CI engine. This has utilised Double Wiebe Function to study the effect of friction power on the engine performance characteristics of a diesel engine by varying different engine parameters such as engine speed, fuel air equivalence ratio, compression ratio and injection timing. The comparison shows good agreement between experimental and simulation results. The study has also yielded two sets of optimum parameters respectively to achieve the maximum engine output and the minimum friction power for the studied engine.

References

[1] I. Wiebe, "Halbempirische formeldur die verbrennungsgeschwindigkeit,"In Kraftstorffaufberitung and Verbrennungbei Diesel Motoren, ed. G. Siotkei, Springer-Verlag, Berlin, 1964, pp. 156–159.

[2] W. T. Lyn, "Calculation of the effect of rate of heat release on the shape of the cylinder pressure diagrams and cycle efficiency," in Proc. Auto Div., Imeche, no. 1, 1960-61.

[3] R. B. Krieger and G. L. Borman, "The computation of apparent heat release for internal combustion engines," ASME paper 66 – WA/DGP– 4, 1966.

[4] A. E. W. Austen and W. T. Lyn "Relation between fuel injection and heat release in a direct injection engine and the nature of combustion process," in Proc. Auto Div. I. MechE, 1960 – 61.

[5] N. D. Whitehouse and R. Way, " Rate of heat release in diesel engines and it's correlation with fuel injection data," in Proc. ImechE, vol. 184, Pt. 3j, 1969–70.

[6] H. C. Grigg and M. H. Syed, "The problem of predicting rate of heat release in diesel engine," in Proc. ImechE, vol. 184, Pt. 3j, 1969– 70

[7] K. Kumar, R. R. Gaur, R. D. Garg, and M. K. Gajendra Babu, "A thermodynamic simulation model for a four stroke medium speed engine," SAE paper no. 840516, 1984.

[8] S. Matsuoka and T. Yoshizaki, "Model verification of burnt gas entrainment spray flame in rapid compression machine: phenomenon and the soot formation mechanism and diesel combustion (free spray flame in rapid compression machine," SAE paper no. 890440, 1989.

[9] N. Miyamoto, T. Chikahiaha, T. Murayama and R. Swayer, R., "Description and analysis of diesel engine rate of combustion and performance using Wiebe's functions," SAE paper no. 850107, 1985.

[10] G. F. Hohensberg "Advanced approaches for heat transfer calculations," SAE 790825, 1979.

[11] Md. Rafiqul Islam, "Studies on the simulation of an alcohol fuelled low heat rejection direct injection engine", Ph. D. Thesis, Dept. of Mechanical Engineering, IIT Delhi, 1992.

[12] Nafis Ahmad, " Use of compressed natural gas in a diesel engine," Ph. D. Thesis, IIT Delhi, 1999.

Appendix: Engine specifications

Engine	: Water-cooled diesel engine
Bore	: 84 mm
Stroke	: 102 mm
CR	: 21:1
Engine speed	: 2000 rev / min.
Displacement volume	: 566 CC
Connecting rod length to crank radius (L/R) ratio	: 4.6 : 1
IVC	: 37^o ABDC
EVO	: 30^o BBDC
Inlet valve diameter	: 0.034 m
Piston skirt length	: 0.0105 m
Piston rings Np	: 2
Suction pressure, SP	: 0.004 bar
Ambient pressure, ambp	: 1.004 bar